INTERACTIVE HEMODYNAMIC SIMULATION MODEL OF A CROSS-SCALE CARDIOVASCULAR SYSTEM

Sarah Hofmann
Andreas Müller
Sebastian von Mammen

Games Engineering, Chair of Human-Computer Interaction
Julius-Maximilians University
Am Hubland, 97074 Würzburg, GERMANY
{sarah.hofmann,andreas.h.mueller,sebastian.von.mammen}@uni-wuerzburg.de

ABSTRACT

Mathematical models of the cardiovascular system (CVS) allow to explore the inner workings of the human body and therefore provide various benefits to medical education. There are indeed some comprehensive models covering complex physiological mechanisms, yet, most of these do not provide the flexibility to change the defining parameters at all times. In this paper, we present CAVA – an interactive, hemodynamic model of a cross-scale CVS that provides just this flexibility, combining the trachea, lung, heart and vascular system approximated as a single vessel. We evaluated the outcome by comparison to empirical measures from literature and analyzed its performance, demonstrating that CAVA is well suited for real-time interactive systems. The code base including examples for two game engines is provided open-source.

Keywords: Cardiovascular, Cross-scale, Cross-compartment, Real-Time Interactive System

1 INTRODUCTION

Since Cardiovascular diseases (CVD) are the leading cause of death worldwide (WHO 2019), the demand for quantitative investigations has increased greatly over the last decades (Quarteroni 2006). A better understanding of CVDs could lead to easier decision-making and improved treatments, eventually resulting in the decrease of clinical costs (Brunberg et al. 2009). A research approach in this context are computational and mathematical simulation models of the human CVS (Broomé et al. 2013). Their aim can range from understanding basic biological systems to generating new hypotheses to patient-specific modeling (Kassab and Guccione 2019). Furthermore, those models could overcome the limitations of studies on humans due to ethical or financial issues (Ishbulatov et al. 2020). However, the realization of an accurate simulation is difficult, as the CVS is highly complex (Quarteroni 2006). A single model can hardly represent all potential events and actions that may occur in the overall system. Especially the geometry of human organs, e.g. the non-linearity of the beating myocardium of the heart, makes it difficult to accurately model the CVS. Nevertheless, a simplified model could still be extremely valuable. Without the necessity to simulate the entire CVS and all its properties, the computation time for simpler models is rather short and therefore they can be a powerful tool for clinical decision-making (Bozkurt 2019). As noted by one reviewer of this paper, there are some advanced comprehensive physiological simulation models, but lack flexibility in adjusting parameters at runtime, enhancing the knowledge about the correlations of bodily functions. Furthermore,

due to their large scope and complexity, examined systems had a relatively high impact on performance. Thus a mathematical, hemodynamic model of the CVS called CAVA has been created, providing just this flexibility at negligible computational cost. CAVA itself is divided into four parts: trachea, lung, heart and vascular system as a single vessel. Section 2 will first introduce the different categories of CVS models. Examples of existing implementations will be presented in section 3. Subsequently, the functionality of CAVA will be elaborated on (section 4), followed by a short evaluation of its behavior and computational cost (section 5). The paper will conclude with a small discussion on the limitations of CAVA in its current state (section 6) and a short outlook on potential future improvements (section 7).

2 MODEL TYPES

In general, models of the human CVS are categorized according to their complexity. Zero-dimensional (0D) models are strongly reduced to basic functions of the human body, whereas models of higher dimension can depict correlations more realistically (Bersani et al. 2017).

2.1 0-Dimensional Models

0D models assume a one-way flow of blood through the organs (Kant and Boswal 2011) with a uniform distribution of essential variables such as blood pressure or volume (Abdi et al. 2015). In particular, all 0D models are governed by ordinary differential equations. These simple models can be further divided into two sub-types: 1-compartment and multi-compartment models. The former consider the systemic vasculature as a whole, entailing that internal pressure distribution and flow velocities in different parts of the vascular network are not calculated separately. In contrast, multi-compartment models include vascular segments as individual compartments containing information on spatial details (Malatos et al. 2016).

2.2 1-Dimensional Models

One-dimensional (1D) models are based on simplified fluid flow equations solved in frequency domain using Fourier or Laplace transformations, which are mostly partial differential equations. A model of this kind can be formed with the help of numerical and analytical methods. Thereby several boundary outflow conditions have to be specified due to the hyperbolic nature of the underlying 1D pulse wave equations. For an instance at the inlet of a blood vessel the pressure and flow rate applied have to be based on derivations or experimental data.(Malatos et al. 2016). With 1D models it is possible to study pulse wave dynamics in arterial segments or even the complete arterial network

2.3 Multi-Scale Models

2D or 3D models, also called multi-scale, combine the efficiency of continuum models with higher fidelity of atomistic and mesoscopic systems. The governing equations, usually based on Navier-Stokes, account for the local vascular geometry, which allows for a more detailed prediction of hemodynamic properties. Theoretically, models of higher dimensions would be superior to simpler models, as they depict the interplay of the human organs more realistically, but to this date even multi-scale models are limited regarding accuracy and required computational power. A common strategy to tackle this issue is to couple 0D models with higher dimensional models to obtain accurate results adapted to specific expectations of the model's behaviour (Malatos et al. 2016, Kassab and Guccione 2019).

3 MODELING EXAMPLES

The majority of models in literature that simulate functions of the CVS cover only single compartments (Bersani et al. 2017) as this allows to focus on their specific workings. Still, there are some multi-compartment models that depict the entire CVS connecting blood flow with oxygen transport (Goldman 2008). For instance, Blanco et al. created a 3D-1D-0D model of the CVS. Herein the arterial tree itself is described as a 1D model, whereas the connection to arterioles and capillaries as well as the circulation of the heart are managed by a 0D model. To further enhance the system, the local hemodynamics of striking blood vessels are upgraded to 3D (Blanco and Feijóo 2010). Broomé et al. created a time dependent multi-compartment model of the heart function, covering the opening and closing of the valves, thereby leading to changes in pressure and various pathological states. Additionally, their model incorporates the calculation of blood oxygen saturation under the assumption that it is homogeneous in every compartment and oxygen transport between compartments is proportional to blood flow (Broomé et al. 2013). Most similar to CAVA there is the Pulse Physiology Engine (Bray et al. 2019), a fork from the BioGears C++ library for body physiology simulations (Baird et al. 2020). Its system is built upon various compartments describing cardiovascular physiology, respiratory physiology, blood chemistry, substance transport and more. Yet, the engine implements mostly lumped parameter models and, in contrast to CAVA, the modification of input parameters is more complicated. The definition of patient-describing properties is done at the initialization phase of the engine, the only intended means of input during runtime is through pre-defined actions. Thus, it is difficult to examine which properties depend on each other or cause drastic changes.

4 CAVA

The functionality of CAVA's CVS is reduced to four compartments: the trachea, the lung, the heart and the vascular system. These organs are modeled with dimensions ranging from 0 to 2. The trachea (0D) is a simple compartment, solely working as an input layer for the lung (1D). The heart (0D) is a multi-compartment model, as it is divided into its four chambers: the respective ventricles and the atria. The blood circuit is modeled as a single blood vessel (2D). In addition, the tissue is implemented as a non-contributing compartment working as a recipient of the vessel's actions. One of the main aims of CAVA is to model the oxygen inflow to the consuming organs represented as the tissue (see fig.1). Thus backflow and transport of emerging carbon dioxide is neglected.

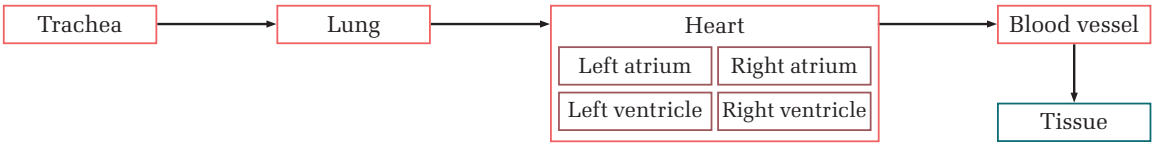

Figure 1: CVS compartments and their interactions in the CAVA model.

4.1 Mathematical Model

All equations of CAVA have been retrieved from previous studies on the individual compartments and combined into one CVS model. Time t in seconds stands for the point of time within the cardiac cycle.

4.1.1 Trachea

The calculated characteristics of the trachea include the tracheal Womersley number W, which is an expression of the pulsatile flow frequency in relation to viscosity, and the tracheal Reynolds number R, which is

used to predict the subsequent flow rate of the air fr_t. To properly compute these values, the cross sectional area a_t is calculated with the help of the tracheal diameter $\delta_t = 18mm$ (Gaddam and Santhanakrishnan 2021) and the outer thickness $t_o = 3mm$ (Furlow and Mathisen 2018). Further, the following tracheal properties are defined: viscosity of air $\eta_t = 1.46 \cdot 10^{-5} \frac{m^2}{s}$, mean speed of air flow $v_{t_m} = 3.4 \frac{m}{s}$, respiratory rate $r_r = 12.5 \frac{breaths}{min}$, duration of the breathing cycle $t_b = \frac{60}{r_r} s$ and duration of inhalation $t_i = 0.5 \cdot t_b$ (Gaddam and Santhanakrishnan 2021). In addition to the following equations the incoming oxygen content is adjusted according to a potential (partial) blockage of the trachea.

$$a_t = 0.25\pi(\delta_t^2 - (\delta_t - 2t_o)^2) \quad (1) \qquad W = \frac{\delta_t}{2 \cdot \sqrt{\frac{2\pi}{t_b \eta_t}}} \quad (2) \qquad R = \frac{v_{t_m} \delta_t}{\eta_t} \quad (3)$$

In the case of exhalation fr_t (4a) is multiplied by the term described in (4b):

$$fr_t = 60 \cdot \frac{a_t \eta_t R}{\delta_t} \quad (4a) \qquad \frac{t_i}{t_b - t_i} \quad (4b)$$

4.1.2 Lung

The characteristics of the lung in CAVA consist of the oxygen flow f_{O_2} and the pressure p_l (Hao et al. 2019). The constant properties are defined as: area of throttle $a_{l_t} = 32mm^2$ (Niu et al. 2017), upstream and downstream pressure $p_u = 41.0mmHg$ and $p_d = 10.3mmHg$ (Smiseth et al. 1999, Hasinoff et al. 1990), critical pressure ratio $\theta = 0.528$, gas constant $G = 287 \frac{J}{kg \cdot K}$ (Hao et al. 2019), lung volume $V_l = 3.251l$ (McDonough et al. 2015), atmospheric density $\rho_a = 1.2 \frac{kg}{m^3}$ (Picard et al. 2008) , body temperature $T = 309.15K$, air mass flow $f_m = 0.12 \frac{kg}{s}$ (Sabz et al. 2019) and mass of air $m_a = 0.03g$ (Calzà et al. 2009). Depending on whether the respiratory status is inhalation or exhalation, the flow coefficient λ_1 is set to 1 or -1 and the respiratory compliance c_{res} to $58 \frac{ml}{cmH_2O}$ or $44 \frac{ml}{cmH_2O}$ respectively (Oikkonen and Tallgren 1995).

$$f_{O_2} = \alpha \frac{a_{l_t} p_u \cdot \sqrt{1-\theta}}{\rho_a \cdot \sqrt{GT}} \cdot \sqrt{1 - (\frac{\frac{p_d}{P_u} - \theta}{1-\theta})^2} \quad (5) \qquad p_l = \frac{f_m G T V_l t}{V_l^2 + c_{res} m_a G T} + \lambda_1 \quad (6)$$

4.1.3 Heart

The properties of the heart in CAVA include the total flow rate f_h, as well as atrial and ventricular specific flow rates (D'Angelo and Papelier 2005). Predefined characteristics of the heart involve the heart rate $r_h = 70 \frac{beats}{min}$, stroke volume $V_{S_h} = 80ml$ (D'Angelo and Papelier 2005) and duration of the heart cycle $t_h = 0.8s$ with two key times for the specific calculations $t_{k_1} = 0.33 \cdot t_h$ and $t_{k_2} = 0.45 \cdot t_h$ (Bozkurt 2019).

$$f_h = V_{S_h} r_h \quad (7)$$

Due to the simplifications of the CVS in CAVA there are no differences in the left and right atrium (LA, RA) for the calculation of the elastance e_a (D'Angelo and Papelier 2005). Only the coefficient λ_2 is of different size: $\frac{1}{3}$ for the LA and $\frac{2}{3}$ for the RA. The atrial properties can then be calculated with the activation

function $\sigma(t)$ and the following preset parameters: minimum and maximum elastance $e_{min} = 0.2\frac{mmHg}{ml}$ and $e_{max} = 0.3\frac{mmHg}{ml}$, the coefficients $\iota = 5.5$ and $\kappa = 1.2$, a specific atrial time in the cardiac cycle $t_{k_3} = 0.04s$ and the radius at zero pressure $r_{p_0} = 1.316cm$ (Cheng et al. 2004). The atrial pressures p_{a_l} and p_{a_r} are calculated as a function of time t. The atrial radii r_{a_l} and r_{a_r} are calculated assuming the atrium being of a spherical shape, dependent on an array of volumes $(V_{v_l}, V_{v_r}, V_{a_l}, V_{a_r})$ that change over time (Bozkurt 2019).

$$\sigma(t) = 1 - \cos 2\pi \frac{t - t_{k_3}}{t_h - t_{k_3}} \tag{8a}$$

$$\sigma(t) = 0 \quad \textbf{if} \quad t_{k_3} \leq t < t_h \tag{8b}$$

$$e_a = e_{min} + 0.5(e_{max} - e_{min}) \cdot \sigma(t) \tag{9}$$

$$p_{a_l} = e_a \iota \kappa \pi \cdot (r_{a_l}^2 - r_{p_0}^2) \cdot \lambda_2 \tag{10}$$

The different volumes of the left and right ventricle (LV, RV) entail different preset values for the ventricular end-systolic elastance $e_{es_l} = 2.5ms$ and $e_{es_r} = 1ms$ and the coefficients $\omega_l = 1.15$ and $\omega_r = 1.75$ (Bozkurt 2019). The ventricular radius $r_{v_{l_{p_0}}}$ at zero pressure is determined as the smallest radius according to the preset volumes. The blood density $\rho_{b_v} = 1.06\frac{g}{cm^3}$ and $\lambda_3 = 1$ are equal in both ventricles and the inflow length t_{l_i} is calculated as the double of the radius. With the aforementioned properties, the inflow inertance I_{v_l} (Broomé et al. 2013), the active, passive and total pressures $p_{v_{l_a}}$, $p_{v_{l_p}}$ and p_{v_l} as well as the radius r_{v_l} are computed in CAVA. $\tau(t)$ is an activation function for the pressure determination (Bozkurt 2019).

$$r_{v_l} = \frac{\frac{3V_{v_l}}{2\pi}}{16\omega_l} + \lambda_3 \tag{11}$$

$$I_{v_l} = \frac{\rho_{b_v} t_{l_i}}{\pi r_{v_l}} \tag{12}$$

$$\tau(t) = \frac{1 + cos\pi \frac{(t - t_{k_1})}{(t_{k_2} - t_{k_1})}}{2} \tag{13a}$$

$$\tau(t) = \frac{1 - cos\pi \frac{t}{t_{k_1}}}{2} \quad \textbf{if} \quad t < t_{k_1} \tag{13b}$$

$$p_{v_{l_a}} = e_{es_l} \cdot 8\pi\omega_l (r_{v_l}^2 - r_{v_{l_{p_0}}}^2) \cdot \tau(t) \tag{14a}$$

$$p_{v_{l_p}} = e^{0.16\pi\omega_l r_{v_l}^2} - 1 \tag{14b}$$

$$p_{v_l} = p_{v_{l_a}} + p_{v_{l_p}} \tag{14c}$$

4.1.4 Blood Circuit

The vascular system of CAVA is modeled as a single blood vessel into which two well-known models of the blood flow are integrated. First, the Windkessel model depicts the blood flow parameters analogous to electrical conductivity. Depending on the requirements of a CVS the Windkessel model can consist of 2, 3 or 4 elements. A 2-element model includes one capacitor for the compliance of large arteries and one resistor for the resistance of small peripheral arteries. Adding one more resistor for the aortic valve to the blood flow forms a 3-element Windkessel model. Making the equations dependent on the cardiac cycle time raises the model to 4 elements. All equations follow basic laws of fluid dynamics (Malatos et al. 2016). The Windkessel model of CAVA can be associated with a 4-element model (see fig. 2).

Another established idea about quantifying oxygen transport at the microcirculatory level integrated in CAVA has been introduced by Krogh. His model describes the mechanism of oxygen exchange between

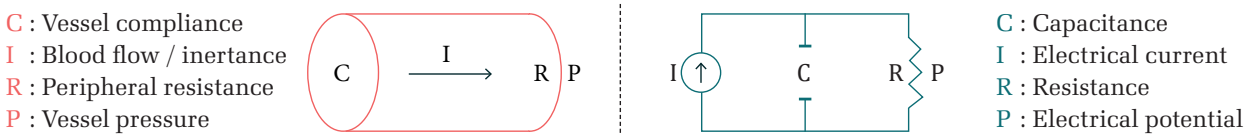

Figure 2: Windkessel model for a blood vessel (left) compared to an electrical circuit (right).

a single capillary and a surrounding cylinder of uniform tissue. Krogh assumed that oxygen is diffused passively, driven by gradients of oxygen tension and uniformly in a radial direction from the blood in the capillary into the tissue. The design is further based on the hypothesis that the blood is a homogeneous fluid and presents no resistance to the diffusion. Therewith, the oxygen consumption rate in the tissue is the same throughout the whole cylindrical volume (Pittman 2011, Possenti et al. 2021). The model has been augmented with the corresponding differential equations governing oxygen diffusion and uptake in a tissue cylinder by Erlang (Popel 1989). Although some of Kroghs assumptions turned out to be incorrect (Secomb 2015), the model is the basis of many modern oxygen transport models (Goldman 2008), as the fundamental idea has been proven to be valid in simplified conditions. This basic cylindric model is depicted in fig. 3.

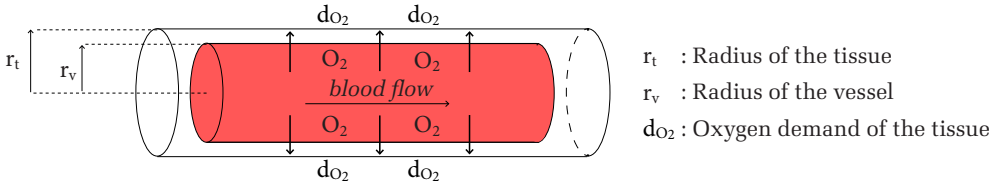

Figure 3: Illustration of the Krogh cylinder model used in CAVA. The arrows labeled with O_2 present the d_{O_2} radial vectors. Based on d_{O_2}, r_v and t_v the partial pressure inside of the cylinder can be computed.

The preset, constant values of the blood vessel's properties required for the velocity v_b and the Windkessel calculations including resistance R_b, inertance I_b, compliance C_b (Abdolrazaghi et al. 2010) and elastance E_b (Broomé et al. 2013) as well as diastolic and systolic pressure P_s and P_d (Choudhury et al. 2014) inside the vessel are defined as follows: start velocity $v_{b_s} = 424.4\frac{mm}{s}$, number of parallel vessels $n_v = 1$ (Secomb 2015), viscosity $\vartheta = 6.72 mPa \cdot s$ (Lowe et al. 1980), Young modulus $Y = 400 kPa$ (Olufsen and Nadim 2003), blood density $\rho_b = 1.06\frac{g}{cm^3}$ (Broomé et al. 2013), coefficients $\lambda_4 = 1$, $\lambda_5 = 0.2057$ and $\lambda_6 = 0.0392$, initial systolic pressure $P_{s_0} = 120 mmHg$ and initial diastolic pressure $P_{d_0} = 80 mmHg$ (Choudhury et al. 2014). The proportions of the blood vessel (Olufsen and Nadim 2003) have been approximated by calculating the mean of vessel radius $r_v = 0.48 cm$ and vessel thickness $t_v = 0.059$. Further, in order to obtain the values of systolic blood pressure, I_0 has to be calculated as a flow-dependent parameter.

$$v_b = 2v_{b_s} \cdot \frac{1-\lambda_4^2}{r_v^2} \quad (15) \qquad R_b = \frac{\lambda_5}{\lambda_6 - 1} \cdot \frac{8\vartheta l_v}{\pi n_v r_v^4} \quad (16) \qquad I_b = \frac{\lambda_5}{\lambda_6} \cdot \frac{8\rho_b l_v}{\pi r_v^2} \quad (17)$$

$$C_b = \frac{3\pi r_v^3 \cdot I_b}{2Y t_v} \quad (18) \qquad E_b = \frac{Y t_v}{2\pi l_v n_v r_v^2} \quad (19) \qquad P_d = P_{d_0} \cdot e^{\frac{-0.75 t_h}{R_b C_b}} \quad (20)$$

$$I_0 = \frac{f_h t_h}{\frac{60 t_h}{\pi}} \quad (21) \qquad P_s = P_{s_0} \cdot e^{\frac{-0.25 t_h}{R_b C_b}} + \frac{\pi t r_v^2 I_0 C_b}{(0.25 t_h)^2 + C_b^2 \pi^2 R_b^2} \cdot (1 + e^{\frac{-0.25 t_h}{R_b C_b}}) \quad (22)$$

The predefined properties of the blood vessel integrated into the Krogh model are as follows: Bunsen solubility coefficient $\beta = 3 \cdot 10^{-5} ml$ (Popel 1989), hemoglobin concentration $c_{Hb} = 13.8\frac{g}{100ml}$ (Christoforides

and Hedley-Whyte 1969), hemoglobin-oxygen saturation $s_{Hb/O_2} = 0.88\%$ (Payen et al. 2009), velocity of red blood cells $v_{rbc} = 2.5\frac{mm}{s}$ (Jeong et al. 2006), oxygen binding capacity $cb_{O_2} = 1.34\frac{ml_{O_2}}{g_{Hb}}$ (Pittman 2011), the metabolic rate $\sigma_{meta} = 4 \cdot 10^{-5}\frac{ml}{s}t$ (Tenney 1974) and Krogh diffusion coefficient $K = 2.41 \cdot 10^{-4}\frac{m^2}{s}$ (Possenti et al. 2021). To obtain the partial pressure PPb inside the Krogh cylinder, first the Hill coefficient H and the half-pressure P_{50} must be computed, both dependent on the body temperature T (Jasiński 2020).

$$H = \begin{cases} 2.57 & \textbf{if } T < 310.15K \\ 2.45 & \textbf{if } T > 317.15K \\ -0.017T + 3.199 & \textbf{else} \end{cases} \quad (23a) \qquad P_{50} = \begin{cases} 27mmHg & \textbf{if } T < 310.15K \\ 35.9mmHg & \textbf{if } T > 317.15K \\ 1.27T - 19.99 & \textbf{else} \end{cases} \quad (23b)$$

$$PP_b = P_{50} \cdot \frac{s_{Hb/O_2}}{1 - s_{Hb/O_2}}^{\frac{1}{H}} \quad (23c)$$

Oxygen flow f_b and concentration c_{O_2} (Pittman 2011, Popel 1989) are determined as follows:

$$f_b = \frac{\pi(2r_v)^2}{4} \cdot v_{rbc} \cdot cb_{O_2} \cdot c_{Hb} \cdot s_{Hb/O_2} \quad (24) \qquad c_{O_2} = \beta \cdot PP_b \quad (25)$$

The partial pressure in the surrounding tissue PP_t can be determined in addition to its oxygen consumption rate $\sigma_{t_{O_2}}$ with the help of the Michaelis-Menten-Formula and the preset value of the tissue's oxygen demand $d_{O_2} = 6.17 \cdot 10^{-5}\frac{ml_{O_2}}{cm^3 \cdot s}$ (Tenney 1974, Possenti et al. 2021):

$$PP_t = PP_b + \frac{\sigma_{meta}}{2K} \cdot \left(\frac{3(r_v^2 - r_t^2)}{8} - \frac{r_t^4}{2(r_v^2 - r_t^2)} \cdot \ln\frac{r_t}{r_v}\right) \quad (26) \qquad \sigma_{t_{O_2}} = d_{O_2}\frac{PP_t}{PP_b + P_{50}} \quad (27)$$

4.2 Implementation

CAVA is implemented as a C++ library and tested with the game engines Unity and Unreal. The library provides all CVS calculations and gives the user the possibility to create a specific human model with a certain age, gender, weight and body temperature. To get an insight on all featured properties of CAVA, an example application has been set up in Windows Forms. Therein, it is possible to adjust the human's parameters during runtime to observe the relations between the CVS properties. The code base and all examples are freely available under the Apache 2.0 license and can be found via link (CAVA 2022).

5 VALIDATION

To examine the correctness of the model the results of the equations for a female in resting state have been exemplary compared to measured values from literature. The contrasting juxtaposition for values that are constant in CAVA can be seen in table 1. To facilitate the validation of properties that are dependent on time, the update rate of the simulation was fixed to one calculation per millisecond. At a heart rate of 60bpm this resulted in 1000 sample data points for each cardiac cycle. Those points were then connected to form the

line diagrams depicted in the figures 4 and 5. One simulation cycle of CAVA takes on average 0.002ms to calculate on any consumer-grade single-core CPU. Thus, even in highly demanding real-time applications like virtual reality simulations with update rates of 90 frames/s, CAVA requires only about 0.02% of the total time budget per frame, which is negligible. In the same scenario, the examined simulation model Pulse Engine (Bray et al. 2019) took 1.2ms on average which would account for at least 10% of the time budget. Depending on other calculations (like in-game physics, animations and AI) this cost may be prohibitive. All constant values in table 1 are in the range of the values retrieved from literature, c_{O_2} is at least close to its comparison. As the range for the values for E_b and C_b is relatively high depending on the size specification of the blood vessel, the outcome at the end of these ranges is not unexpected. Also, the simplification to only one blood vessel may lead to small deviations. Still, it can be concluded that CAVA is capable to simulate these properties, given a resting condition of the human. Compared to the chart in the original paper (Hao et al. 2019) oxygen flow f_{O_2} is not time dependent but simplified to a constant value and the pressure p_l of the lung shows only a small, almost linear increase. e_a is within the value range measured by (Bozkurt 2019), yet whether the course of the curve is accurate can not be validated with the examined paper. Small deviations of the ventricular radii r_{v_l} and r_{v_r} from the original charts in (Bozkurt 2019) can be attributed to the fact that the volumes for the chambers have been approximated and divided in several time steps, thus the charts show also a gradual increase. The ventricular pressures p_{v_l} and $p_{v_{rl}}$ depend on the calculation of these radii, therefore deviations can be seen as an subsequent error. Yet overall, the pressure curves are quite similar to the original. The charts for r_{a_l}, r_{a_r}, p_{a_l} and p_{a_r} do not exactly replicate the original charts, but there are no unrealistic spikes, therefore it is acceptable. Deviations can also be attributed to only approximated atrial volumes over time. The equations for diastolic and systolic pressure are very close to the expected $120/80$, yet this outcome should be interpreted with caution, as the authors tested the calculations within a 2-element Windkessel model (Choudhury et al. 2014). Further the input values of resistance and compliance have been approximated with multilinear regression, whereas CAVA used the previously calculated values of R_b and C_b multiplied with constants as a simplification.

Table 1: Comparison of the constant parameter values in CAVA to ones obtained from literature. Some of the values from literature show ranges from charts, therefore these limits are only approximated.

Parameter Name	**CAVA**	**Literature**	**Unit**	**Reference**
fr_t (Tracheal flow rate)	28.83	$0-60$	L/min	Gaddam and Santhanakrishnan (2021)
f_{O_2} (Lung oxygen flow)	$2.7 \cdot 10^{-5}$	-60 – 50	L/min	Hao et al. (2019)
f_h (Heart flow rate)	5.6	$5-6$	L/min	D'Angelo and Papelier (2005)
I_v (Ventricular inertance)	0.67	$0-8$	g/cm^2	Flachskampf et al. (1993)
v_b (Blood velocity)	836.24	$100-2000$	$\mu m/s$	Secomb (2015)
C_b (Compliance)	0.04	$0.12-49.5$	$ml/mmHg$	Lim et al. (2013)
R_b (Resistance)	0.7	$0.01-0.95$	$mmHg \cdot s/ml$	Bozkurt (2019)
E_b (Elastance)	18.79	< 18.8	$mmHg/ml$	Lim et al. (2013)
I_b (Inertance)	0.019	$0.013-0.055$	$mmHg \cdot s^2/ml$	Stergiopulos et al. (1999)
c_{O_2} (O_2 concentration)	0.002	~ 0.003	ml_{O_2}/ml_{blood}	Popel (1989)
PP_t , PP_b (Partial pressure)	59.96	$1-100$	$mmHg$	Jasiński (2020)
$\sigma_{t_{O_2}}$ (O_2 consumption)	$4.3 \cdot 10^{-5}$	$< 6.17 \cdot 10^{-5}$	$ml_{O_2}/cm^3 s$	Possenti et al. (2021)
P_d (Diastolic pressure)	$77-80$	< 100	$mmHg$	Choudhury et al. (2014)
P_s (Systolic pressure)	117	< 160	$mmHg$	Choudhury et al. (2014)

6 CONCLUSION

In this paper, we (1) presented a mathematical, hemodynamic cardiovascular model consisting of four compartments (trachea, lung, heart and vascular system) as well as (2) evaluated its mechanism by comparing the

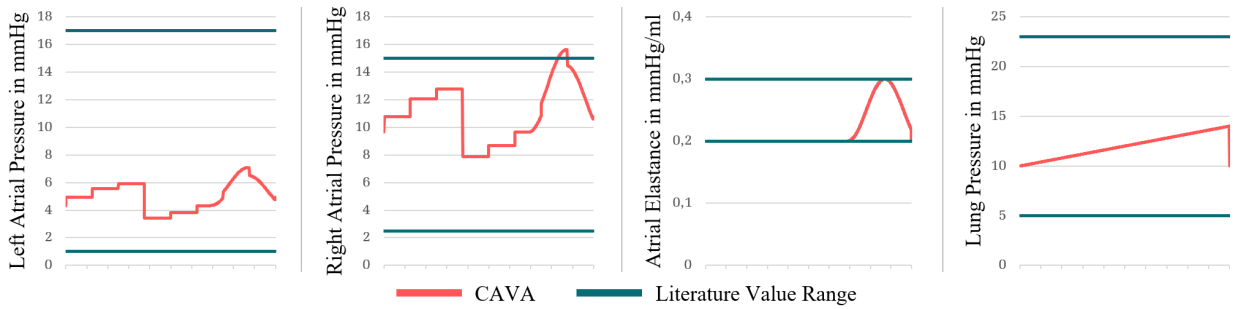

Figure 4: Measured values of atria and lung over the time of one cardiac cycle compared to literature.

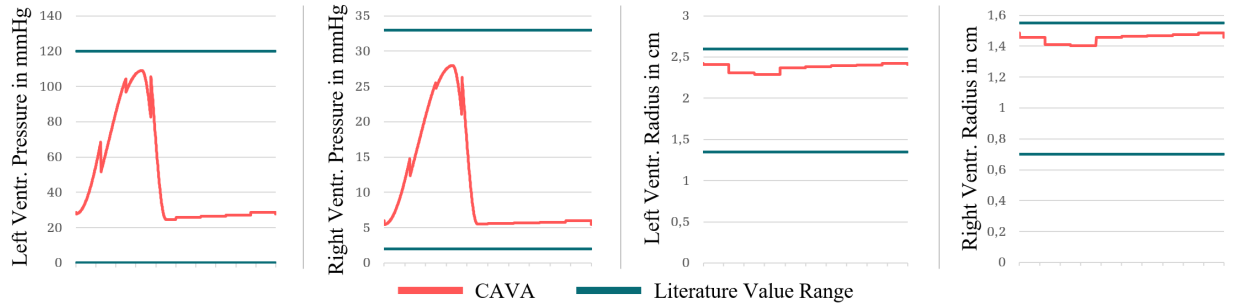

Figure 5: Measured values of ventricles over the time of one cardiac cycle compared to literature.

resulting values to empirical measures from literature. The flexibility and performance of the open-source implementation makes it most suitable for the application in real-time interactive systems. As seen in table 1, for most properties the outcome of CAVA's calculations is close to the values from literature. Yet, as these do not change over time, it can not be guaranteed that the outcome is stable under varying conditions. Further, the constant input values that would normally be time-dependent can sometimes lead to deviations. Since not all processes of the compartments affect each other, extending them with corresponding equations would increase CAVA's accuracy. Also, the simplification of the blood circuit to a single vessel cannot cover the complexity of a real human's circuit. It would be beneficial to separate this compartment into smaller parts like arteries or capillaries. Additionally, only few values are fitted to the set up human so far, this presents another limitation of CAVA that needs to be addressed. Overall, despite the promising results of CAVA's current state there is still room for improvement which will be discussed in the following section.

7 FUTURE WORK

CAVA could be integrated into applications that focus on the interactive simulation of bodily functions such as serious games for health education. The characteristics of a patient in a virtual reality game for first aid training could for example be efficiently simulated in real-time via CAVA. Due to its modular and light-weight architecture, the CAVA library could be easily extended and made more flexible and adaptive to individual human characteristics in order to provide more realistic scenarios. Because of its high computational efficiency and portability, CAVA could be integrated into wearable embedded systems to enrich the simulation with real-time sensor data. Further, the simulation could be extended to not only reflect healthy patients but also account for various diseases that manifest themselves in deviations of processes and resulting physiological health values. It is intended to further validate the functionality especially regarding the simulation of internal and external influence factors like diseases by generating data on a bigger variety of humans and conducting expert interviews. Surely, the current and future scientific progress will allow for a better insight in the CVS, whereby CAVA can be improved upon.

ACKNOWLEDGMENTS

This research was partially funded by the German Federal Ministry of Education and Research (BMBF) as part of the research initiative for Human-Technology Interaction 'Digital Platforms: Interactive Assistance Systems for Humans' in the project VIA-VR (project number 16SV8444).

REFERENCES

Abdi, M., A. Karimi, M. Navidbakhsh, G. Pirzad Jahromi, and K. Hassani. 2015. "A Lumped Parameter Mathematical Model To Analyze The Effects Of Tachycardia And Bradycardia On The Cardiovascular System". *International Journal of Numerical Modelling: Electronic Networks, Devices and Fields* vol. 28 (3), pp. 346–357.

Abdolrazaghi, M., M. Navidbakhsh, and K. Hassani. 2010. "Mathematical Modelling And Electrical Analog Equivalent Of The Human Cardiovascular System". *Cardiovascular Engineering* vol. 10 (2), pp. 45–51.

Baird, A., M. McDaniel, S. A. White, N. Tatum, and L. Marin. 2020. "BioGears: A C++ Library For Whole Body Physiology Simulations". *Journal of Open Source Software* vol. 5 (56), pp. 2645.

Bersani, A. M., E. Bersani, and C. De Lazzari. 2017. "Interaction Between The Respiratory And Cardiovascular System: A Simplified 0-D Mathematical Model". *Cardiovascular and Pulmonary Artificial Organs: Educational Training Simulators. CNR Edizioni*, pp. 87–103.

Blanco, P. J., and R. A. Feijóo. 2010. "A 3D-1D-0D Computational Model For The Entire Cardiovascular System". *Mecánica Computacional* vol. 29 (59), pp. 5887–5911.

Bozkurt, S. 2019. "Mathematical Modeling Of Cardiac Function To Evaluate Clinical Cases In Adults And Children". *PloS one* vol. 14 (10), pp. e0224663.

Bray, A., J. B. Webb, A. Enquobahrie, J. Vicory, J. Heneghan, R. Hubal, S. TerMaath, P. Asare, and R. B. Clipp. 2019. "Pulse Physiology Engine: An Open-Source Software Platform For Computational Modeling Of Human Medical Simulation". *SN Comprehensive Clinical Medicine* vol. 1 (5), pp. 362–377.

Broomé, M., E. Maksuti, A. Bjällmark, B. Frenckner, and B. Janerot-Sjöberg. 2013. "Closed-Loop Real-Time Simulation Model Of Hemodynamics And Oxygen Transport In The Cardiovascular System". *Biomedical engineering online* vol. 12 (1), pp. 1–20.

Brunberg, A., S. Heinke, J. Spillner, R. Autschbach, D. Abel, and S. Leonhardt. 2009. "Modeling And Simulation Of The Cardiovascular System: A Review Of Applications, Methods, And Potentials". *Biomedical Engineering / Biomedizinische Technik (BMT)* vol. 54 (5).

Calzà, G., L. Gratton, T. Lòpez-Arias, and S. Oss. 2009. "Rubber Balloons, Buoyancy And The Weight Of Air: A Look Inside". *Physics Education* vol. 44 (1), pp. 91.

CAVA 2022. "CAVA". https://github.com/zacharina/cava. Accessed Jun. 24, 2022.

Cheng, R., Y. G. Lai, and K. B. Chandran. 2004. "Three-Dimensional Fluid-Structure Interaction Simulation Of Bileaflet Mechanical Heart Valve Flow Dynamics". *Ann. Biomed. Eng.* vol. 32 (11), pp. 1471–1483.

Choudhury, A. D., R. Banerjee, A. Sinha, and S. Kundu. 2014. "Estimating Blood Pressure Using Windkessel Model On Photoplethysmogram". In *2014 36th Annual International Conference of the IEEE Engineering in Medicine and Biology Society*, pp. 4567–4570.

Christoforides, C., and J. Hedley-Whyte. 1969. "Effect Of Temperature And Hemoglobin Concentration On Solubility Of O2 In Blood.". *Journal of applied physiology* vol. 27 (5), pp. 592–596.

D'Angelo, C., and Y. Papelier. 2005. "Mathematical Modelling Of The Cardiovascular System And Skeletal Muscle Interaction During Exercise". In *ESAIM: Proceedings*, Volume 14, pp. 72–88. EDP sciences.

Flachskampf, F. A., L. Rodriguez, C. Chen, J. L. Guerrero, A. E. Weyman, and J. D. Thomas. 1993. "Analysis Of Mitral Inertance: A Factor Critical For Early Transmitral Filling". *Journal of the American Society of Echocardiography* vol. 6 (4), pp. 422–432.

Furlow, P. W., and D. J. Mathisen. 2018. "Surgical Anatomy Of The Trachea". *Annals of cardiothoracic surgery* vol. 7 (2), pp. 255.

Gaddam, M. G., and A. Santhanakrishnan. 2021. "Effects Of Varying Inhalation Duration And Respiratory Rate On Human Airway Flow". *Fluids* vol. 6 (6), pp. 221.

Goldman, D. 2008. "Theoretical Models Of Microvascular Oxygen Transport To Tissue". *Microcirculation* vol. 15 (8), pp. 795–811.

Hao, L., Y. Shi, M. Cai, S. Ren, Y. Wang, H. Zhang, and Q. Yu. 2019. "Dynamic Characteristics Of A Mechanical Ventilation System With Spontaneous Breathing". *IEEE Access* vol. 7, pp. 172847–172859.

Hasinoff, I., J. Ducas, U. Schick, and R. M. Prewitt. 1990. "Pulmonary Vascular Pressure-Flow Characteristics In Canine Pulmonary Embolism". *Journal of Applied Physiology* vol. 68 (2), pp. 462–467.

Ishbulatov, Y. M., A. S. Karavaev, A. R. Kiselev, M. A. Simonyan, M. D. Prokhorov, V. I. Ponomarenko, S. A. Mironov, V. I. Gridnev, B. P. Bezruchko, and V. A. Shvartz. 2020. "Mathematical Modeling Of The Cardiovascular Autonomic Control In Healthy Subjects During A Passive Head-up Tilt Test". *Scientific reports* vol. 10 (1), pp. 1–11.

Jasiński, M. 2020. "Numerical Analysis Of The Temperature Impact To The Oxygen Distribution In The Biological Tissue". *Journal of Applied Mathematics and Computational Mechanics* vol. 19 (3), pp. 17–28.

Jeong, J. H., Y. Sugii, M. Minamiyama, and K. Okamoto. 2006. "Measurement Of RBC Deformation And Velocity In Capillaries In Vivo". *Microvascular research* vol. 71 (3), pp. 212–217.

Kant, S., and T. Boswal. 2011. "Mathematical Model Of Oxygen Transport In Micro Vessels Of Human Body With Special Role Of Blood". In *Proceedings of the National Workshop-cum-Conference on Recent Trends in Mathematics & Computing*, pp. 117–123. Citeseer.

Kassab, G., and J. Guccione. 2019. "Mathematical Modeling Of Cardiovascular Systems: From Physiology To The Clinic". *Frontiers in physiology* vol. 10, pp. 1259.

Lim, E., G. S. Chan, S. Dokos, S. C. Ng, L. A. Latif, S. Vandenberghe, M. Karunanithi, and N. H. Lovell. 2013. "A Cardiovascular Mathematical Model Of Graded Head-Up Tilt". *PloS one* vol. 8 (10), pp. e77357.

Lowe, G., M. M. Drummond, A. Lorimer, I. Hutton, C. Forbes, C. Prentice, and J. Barbenel. 1980. "Relation Between Extent Of Coronary Artery Disease And Blood Viscosity.". *Br Med J* vol. 280 (6215), pp. 673–674.

Malatos, S., A. Raptis, and M. Xenos. 2016. "Advances In Low-Dimensional Mathematical Modeling Of The Human Cardiovascular System". *J Hypertens Manag* vol. 2 (2), pp. 1–10.

McDonough, J. E., L. Knudsen, A. C. Wright, W. M. Elliott, M. Ochs, and J. C. Hogg. 2015. "Regional Differences In Alveolar Density In The Human Lung Are Related To Lung Height". *Journal of Applied Physiology* vol. 118 (11), pp. 1429–1434.

Niu, J., Y. Shi, Z. Cao, M. Cai, W. Chen, J. Zhu, and W. Xu. 2017. "Study On Air Flow Dynamic Characteristic Of Mechanical Ventilation Of A Lung Simulator". *Science China Technological Sciences* vol. 60 (2), pp. 243–250.

Oikkonen, M., and M. Tallgren. 1995. "Changes In Respiratory Compliance At Laparoscopy: Measurements Using Side Stream Spirometry". *Canadian journal of anaesthesia* vol. 42 (6), pp. 495–497.

Olufsen, M. S., and A. Nadim. 2003. "On Deriving Lumped Models For Blood Flow And Pressure In The Systemic Arteries". In *Computational Fluid and Solid Mechanics 2003*, pp. 1786–1789. Elsevier.

Payen, D., C. Luengo, L. Heyer, M. Resche-Rigon, S. Kerever, C. Damoisel, and M. R. Losser. 2009. "Is Thenar Tissue Hemoglobin Oxygen Saturation In Septic Shock Related To Macrohemodynamic Variables And Outcome?". *Critical Care* vol. 13 (5), pp. 1–11.

Picard, A., R. Davis, M. Gläser, and K. Fujii. 2008. "Revised Formula For The Density Of Moist Air (CIPM-2007)". *Metrologia* vol. 45 (2), pp. 149.

Pittman, R. N. 2011. "Oxygen Gradients In The Microcirculation". *Acta Physiol.* vol. 202 (3), pp. 311–322.

Popel, A. S. 1989. "Theory Of Oxygen Transport To Tissue". *Crit. Rev. Biomed. Eng.* vol. 17 (3), pp. 257.

Possenti, L., A. Cicchetti, R. Rosati, D. Cerroni, M. L. Costantino, T. Rancati, and P. Zunino. 2021. "A Mesoscale Computational Model For Microvascular Oxygen Transfer". *Annals of Biomedical Engineering* vol. 49 (12), pp. 3356–3373.

Quarteroni, A. 2006. "What Mathematics Can Do For The Simulation Of Bood Circulation". *MOX Report*.

Sabz, M., R. Kamali, and S. Ahmadizade. 2019. "Numerical Simulation Of Magnetic Drug Targeting To A Tumor In The Simplified Model Of The Human Lung". *Computer Methods and Programs in Biomedicine* vol. 172, pp. 11–24.

Secomb, T. W. 2015. "Krogh-Cylinder And Infinite-Domain Models For Washout Of An Inert Diffusible Solute From Tissue". *Microcirculation* vol. 22 (1), pp. 91–98.

Smiseth, O. A., C. R. Thompson, K. Lohavanichbutr, H. Ling, J. G. Abel, R. T. Miyagishima, S. V. Lichtenstein, and J. Bowering. 1999. "The Pulmonary Venous Systolic Flow Pulse—Its Origin And Relationship To Left Atrial Pressure". *Journal of the American college of Cardiology* vol. 34 (3), pp. 802–809.

Stergiopulos, N., B. E. Westerhof, and N. Westerhof. 1999. "Total Arterial Inertance As The Fourth Element Of The Windkessel Model". *American Journal of Physiology-Heart and Circulatory Physiology* vol. 276 (1), pp. H81–H88.

Tenney, S. 1974. "A Theoretical Analysis Of The Relationship Between Venous Blood And Mean Tissue Oxygen Pressures". *Respiration physiology* vol. 20 (3), pp. 283–296.

WHO 2019. "Cardiovascular Diseases (CVDs) – Key facts". https://www.who.int/news-room/fact-sheets/detail/cardiovascular-diseases-(cvds). Accessed Jul. 23, 2021.

AUTHOR BIOGRAPHIES

SARAH HOFMANN is a Computer Science graduate student and Research Assistant at the Games Engineering group at the Julius-Maximilians University, Würzburg. Her research interests are Interactive Simulations for the Life Sciences.

ANDREAS MÜLLER is a PhD student at the Games Engineering group at the Julius-Maximilians University, Würzburg. His research interests are Real-Time Interactive Systems and Artificial Intelligence.

SEBASTIAN VON MAMMEN is professor of Games Engineering at the Julius-Maximilians University, Würzburg. He completed his habiliation on Interactive Self-Organisation at the University of Augsburg in 2016, his PhD at the University of Calgary in 2009, and his graduate studies in Computer Science at the University of Erlangen in 2005. His research interests are Real-Time Interactive Systems, Interactive Simulation, Artificial Life, and Artificial Intelligence.